

μ -SYNTHESIS FOR UNMANNED UNDERWATER VEHICLES CURRENT DISTURBANCE REJECTION

Eric Conrado de Souza
e-mail: eric.souza@poli.usp.br

Newton Maruyama
e-mail: maruyama@usp.br

Av. Prof. Mello Moraes n.2231, Depto. de Engenharia Mecatrônica e de Sistemas Mecânicos, Escola Politécnica, Universidade de São Paulo, 05508-900, São Paulo, SP, Brasil

Abstract: *This note focuses attention on a novel approach to disturbance rejection when the μ -synthesis control methodology is applied to Unmanned Underwater Vehicles (UUVs). Environmental external disturbances simplifies to ocean current for a totally submerged vehicle and greatly contributes for hydrodynamical loads and the tether cable disturbance. Our case scenario deals with the incorporation of the sea current disturbance to the plant model employed for control design. In the proposed design methodology we substitute the structured unmodeled dynamics uncertainty, which is generally difficult to come up with and eventually utilized to represent external disturbances, by parametric uncertainty, relatively easier and straightforward to come by. The sea-current load parameters are therefore treated as parametric uncertainty and fit in the μ design framework. Assuming both vehicle motion and current direction lie in the horizontal plane, the incoming (to vehicle) current vector sets a horizontal circumference sector in which it may vary. When in the 3D space, current uncertainty renders a cone in space. For validation purposes, the linear controller is simulated with the nonlinear vehicle model.*

Keywords: *Mobile robots, Nonlinear control systems*

1 Nomenclature

M - Generalized mass matrix ($M \in \mathbb{R}^{6 \times 6}$);

$\nu = [u, v, w, p, q, r]^T$ - Velocity vector in body coordinate system ($\nu \in \mathbb{R}^6$);

ν_c - Current velocity vector in body coordinate system ($\nu_c \in \mathbb{R}^6$);

$\eta = [x, y, z, \phi, \theta, \psi]^T$ - Position/attitude vector in inertial coordinate system ($\eta \in \mathbb{R}^6$);

$\tau = [X, Y, Z, K, M, N]$ - Control effort vector in body coordinate system ($\tau \in \mathbb{R}^6$);

$P(s)$ - Augmented Plant Transfer Function;

$\mathcal{F}_{(i)}(A, B)$ - LFT of A and B . $i = \{l(\text{lower}), u(\text{upper})\}$.

subscript

c - Relative to current;

RB - Relative to Rigid Body dynamics;

A - Relative to Added Mass dynamics.

2 Introduction

The success of controlling a system is directly connected to the designer's ability on obtaining an estimate and the relevancy of what is not or is poorly known. The resulting uncertainty model if unstructured may yield conservative designs by leaving out wanted performance. Obtaining a structured uncertainty, which in principle should be more representative, can be exhaustively difficult. Earlier results (Campa et al., 1998) point out relevant issues in regard to structured uncertainty modeling, however, much still remains yet to be done in this regard. In a recent study (Souza et al., 2004) the robust multivariable linear control technique LQG/LTR , applied for Autonomous Underwater Vehicle (AUV) dynamical positioning, considered unmodeled dynamic uncertainty and parametric plant perturbation dwelt by the same control specification, which could render a conservative design. In addition, specifying unmodeled dynamics, even if structured, may not prove to be an easy task. To overcome this difficulty this note focuses attention on transforming what could be considered external disturbance into "easily" modeled parametric perturbation.

Environmental external disturbances simplifies to ocean current for a totally submerged vehicle and greatly contributes for hydrodynamical loads and the tether cable disturbance. By considering AUVs, the μ -synthesis control methodology, applied for velocity control disturbance rejection, here deals with the incorporation of the sea current disturbance to the plant model employed for control design. In the proposed design methodology we substitute the structured uncertainty due to unmodeled dynamics, which is generally difficult to come up with and eventually utilized to represent external disturbances, by structured parametric uncertainty, relatively easier and straightforward to come by. The sea-current load parameters are therefore treated as parametric uncertainty

and fit in the μ design framework. Assuming both vehicle motion and current direction lie in the horizontal plane, the incoming (to vehicle) current vector sets a horizontal circumference sector in which it may vary. When the vehicle moves in the 3D space, the current uncertainty renders a cone in space. System sensitivity with respect to parameter spaces may be verified according to these two cases. For validation purposes, the linear controller is simulated with the nonlinear vehicle model.

This text is organized as follows. System modeling is addressed in Section 3. A brief overview of the μ – *synthesis* control strategy is then presented in Section 4. In the following section, a few controller design issues are considered and some synthesis results are depicted. A quick discussion on fundamental issues such as stability, performance and computational implementation is also made. Simulation results are presented in Section 6. Finally concluding remarks are drawn based on what has been presented and a short review for future implementations is presented.

3 System Modeling

3.1 Vehicle Modeling

The model used in the following discussion is based on the MURS 300 Mark II ROV (Ishidera et al., 1986). Although our discussions are AUV oriented, control design is realized with the MURS 300 vehicle model due to its complete hydrodynamical drag coefficient data available. This assertion is supported by the fact that we will be restricting our model based control design to relatively low velocities and, so, ROV and AUV dynamics can be considered similar, when neglecting the ROV tether cable loads. The MURS 300 vehicle is nearly neutrally buoyant and controllable on all six degrees of freedom (*dof*). It is propelled by six thrusters distributed longitudinally two by two on each body axis. A full order mathematical model has been developed, i.e., all six degrees of freedom are considered.

The underwater vehicle is modeled by standard and well established general dynamics which may be formulated according to the following nonlinear and coupled expression (Kalske and Haponen, 1991; Fossen, 1994; Souza, 2003):

$$M\dot{\nu} + C(\nu)\nu + F_D(\nu_r) + G(\eta) = \tau_{prop} + \tau_c, \quad (1)$$

$$\dot{\eta} = J(\eta)\nu \quad (2)$$

where:

$$M = M_{RB} + M_A \quad \text{and} \quad C(\nu) = C_{RB}(\nu) + C_A(\nu). \quad (3)$$

The generalized mass matrix M accounts for vehicle inertia the inertia matrix M_{RB} and the added (A) mass inertia matrix M_A , modeled as diagonal. It is important to make note that added mass coefficients may be considered constant for a totally submerged vehicle at a depth where the influence of waves is not minimal. Likewise, the centripetal and Coriolis force matrix C is derived from the rigid body the centripetal and Coriolis force matrix C_{RB} are derived from the rigid body (RB) dynamic expressions and also includes the centripetal and Coriolis force matrix C_A , which derive from Kirchhoff's equations, see (Fossen, 1994). The term $F_D(\nu_r)$ stands for nonlinear hydrodynamic damping action. It is important to observe that in Eq. 1 the hydrodynamic drag is a function of the relative velocity ν_r , which is obtained by the vehicle orientation with respect to fluid motion or current ν_c , i.e., the hydrodynamic coefficients in $F_D(\nu_r)$ vary with the vehicle state and current orientation. That is:

$$\nu_r = \nu - \nu_c. \quad (4)$$

Lift force components are considered negligible for non-wing-like vehicles and when are restricted to operating with moderate velocity profiles. Restoring forces and moments are accounted for in $G(\eta)$, comprising gravitational weight and buoyancy components. The current disturbance is given by τ_c and other environmental phenomena are not considered. When considering neutrally buoyant vehicles with homogeneously distributed mass, Eq. 1 may be written with respect to the relative velocity ν_r by switching τ_c to the left side of the equality sign and plugging it to the vehicles dynamics in $M\dot{\nu}$ and $C(\nu)\nu$. τ_{prop} denote propulsion activity. The J matrix indicates when coordinate transformation is made between the inertial and mobile reference coordinate frames.

The approach for current disturbance rejection adopted here considers the assumption described above, except that instead of writing the overall vehicle dynamics with respect to the relative velocity ν_r , the current velocity dependent terms are considered as system parameters that may vary slowly in time. This enables the μ control methodology implementation for *LTI* systems. System state remains the vehicle velocity ν . By proceeding in this manner, the “external” current disturbance, which would initially be modeled as a frequency dependent unmodeled dynamics uncertainty and sometimes difficult to come up with, is transformed to plant parametric perturbation, much more easily identified by simply specifying the interval of coefficient variation or, in this case, of current data. More details are given in what follows.

3.2 Model Linearization

The system new state vector is chosen to equal velocity vector. The linear system was obtained by classical or Jacobian linearization, around nominal velocity values of $\nu_1 = [1.0; 0.1; 0.1]m/s$ and $\nu_2 = [0.1; 0.1; 0.1]rad/s$, yields the state matrix A and the input matrix B . The output matrix $C = I_6$ was chosen so the output y reflects only the linear and angular velocity vector ν . The resulting linear system is minimum phase, slightly unstable, and was tested and confirmed for controllability and observability.

3.3 Variable Scaling

This procedure may be carried out by employing maximum values of the output y , and the input u (or state x) of the linear plant model in the following manner:

$$\bar{G}(s) = G_{norm}(s) = S_y^{-1}G(s)S_u. \quad (5)$$

The scaling variables usually are obtained by employing nominal output $y = \nu$ and input $u = \tau$ values or expected maximum values. In this case, the scaling matrices are given as:

$$S_y = \text{diag}\{u_{max}, v_{max}, w_{max}, p_{max}, q_{max}, r_{max}\}, \quad (6)$$

$$S_u = \text{diag}\{X_{max}, Y_{max}, Z_{max}, K_{max}, M_{max}, N_{max}\}. \quad (7)$$

As a direct consequence of this normalization the singular values of the system are drawn closer together, frequency-by-frequency, and so are the Bode plots for the singular value curves. Instead of considering variable scaling by maximum values, the scaling procedure, however, was obtained by fully automating a search process, in the frequency domain, by iterating the scaling matrices. Nominal or maximum output and input entries may be used as a boundary condition. The search algorithm stops when the local minimum is found. This procedure was found to be more efficient than the former alternative.

3.4 Uncertainty Characterization

It is important to stress out that the uncertainty relative to the generalized mass matrix M complies real physical parameters, of the added mass coefficients of M_A , since the uncertainty is relative only to the added mass coefficients, and not to the vehicle's mass, center of mass or moments of inertia. The uncertainty with respect to the hydrodynamic block HD , of Fig 4, is described below.

A system physical parameter, i.e. hydrodynamical, uncertainty in the HD block representation was not performed due to difficulty in expressing the LFT of the complex hydrodynamic drag dynamical model, composed of trigonometric and high degree polynomial coefficient functions with respect to vehicle attitude in the current. Instead of physical parameter uncertainty modeling, the alternative of calculating the final maximum and minimum dynamical values was used. In other words, by considering current and added mass variation, the maximum and minimum values of their hydrodynamic dependent terms were obtained and with these parametric uncertainty could be specified. More on this is explained in Section 5.

To all added mass coefficients it was attributed a 10% relative uncertainty. As stated before, in the methodology here implemented the current is not considered an external disturbance but belongs to the vehicle model. Thus, the current vector also has a 10% variation interval relative to its magnitude. In addition, the current vector had an 5° uncertainty on its nominal orientation. Moreover, each hydrodynamic drag coefficient, which is a function of the vehicles velocity and current, also have an associated 10% relative uncertainty. Since uncertainty in this context is only attributed to hydrodynamical dynamics, rigid body expressions have no related uncertainty, and, therefore, need not be a LFT .

Initial designs were used for testing. The purpose of testing is twofold: gain insight on the control methodology and to serve as an initial system modeling for the final controller synthesis.

When all parameters were treated as real uncertainty scalars the lower μ bound showed to be very discontinuous, despite the complex sensitivity performance specification. On the other hand, when considering only the generalized mass uncertainty as complex, the lower μ bound function was found to be "smooth" or continuous over the entire frequency range, similar to results obtained when only complex uncertainty was considered.

4 μ - Synthesis Methodology Overview

As stated before, the μ -synthesis is here implemented. A brief overview on the μ -synthesis controller design methodology is made below. From Fig. 2(a), the design objective is to find a stabilizing controller K such that for all uncertainty Δ the closed-loop system is stable and satisfies

$$\|\mathcal{F}_u[\mathcal{F}_l(P, K), \Delta]\|_\infty = \|\mathcal{F}_l[\mathcal{F}_u(P, \Delta), K]\|_\infty < 1, \quad (8)$$

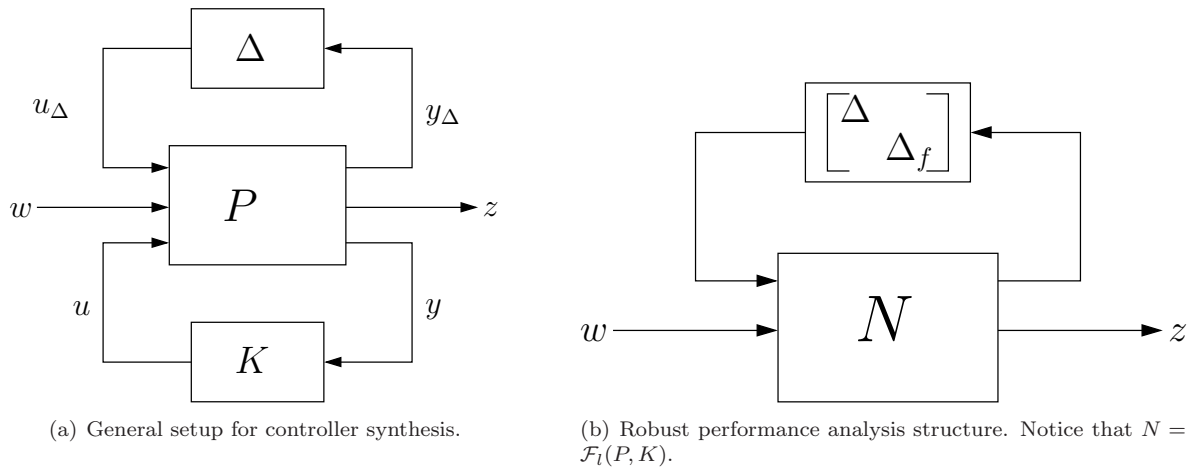


Figure 2. Robust control synthesis.

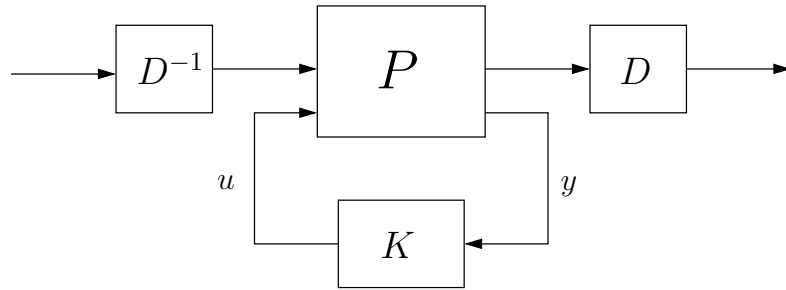


Figure 3. Control synthesis via D -scaling matrices.

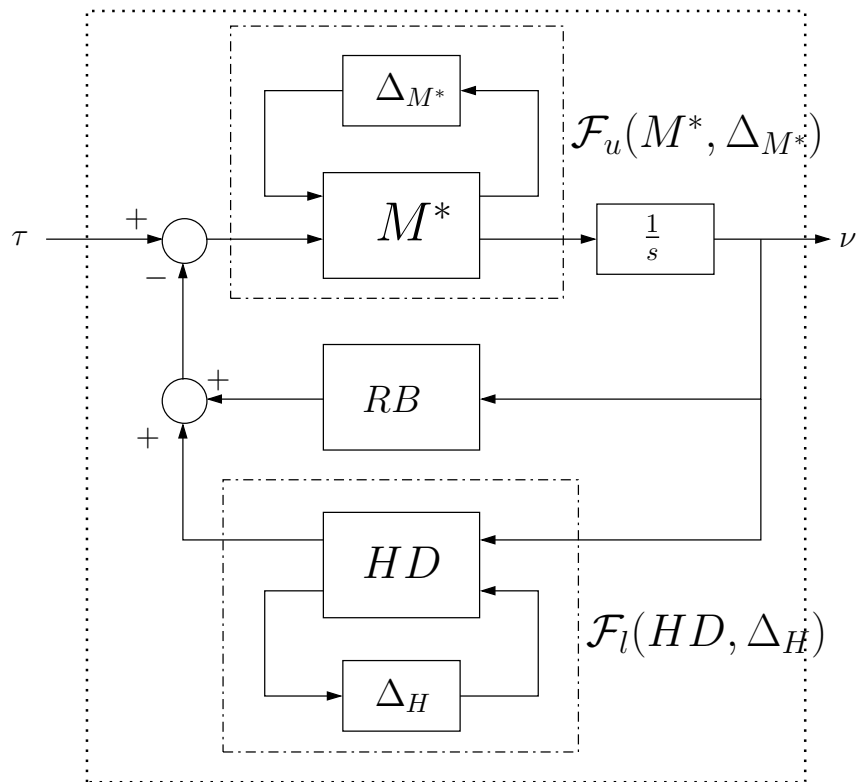


Figure 4. Plant LFT and uncertainty representation. The RB block stands for rigid body linear expression without an associated uncertainty.

The generalized mass matrix uncertainty is restricted to the added mass coefficients. For example: for the added mass matrix

$$M_A = \text{diag}\{X_{\dot{u}}, Y_{\dot{v}}, Z_{\dot{w}}, K_{\dot{p}}, M_{\dot{q}}, N_{\dot{r}}\}, \quad (13)$$

the hydrodynamic uncertainty refers to each *dof* physical added mass coefficient, and, therefore, considering only the *surge* direction:

$$X_{\dot{u}} = \bar{X}_{\dot{u}} + p_{X_{\dot{u}}} \bar{X}_{\dot{u}} \delta_{X_{\dot{u}}}, \quad |\delta_{X_{\dot{u}}}| \leq 1 \quad (14)$$

where $\bar{X}_{\dot{u}}$ is the mean added mass value, $p_{X_{\dot{u}}}$ is the percentage measure of relative uncertainty and $\delta_{X_{\dot{u}}}$ is the scalar coefficient uncertainty. In contrast, due to the difficulty in posing a *LFT* representation for parameters that enter trigonometric and complex polynomial functions, the uncertainty of the hydrodynamic efforts of block *HD* were not obtained in the same manner. As mentioned in the end of Section 3, the procedure here adopted renders a *LFT* of the general hydrodynamical *HD* block for every matrix element. The extremal values or worst case current and hydrodynamical uncertainty was obtained by a semi-automated algorithm, implemented in MATLAB, where maximum and minimum, or worst case, values were obtained for the generalized *LFT* of the M^* and *HD* blocks of Fig. 4.

5.2 Performance Specification

The weighted sensitivity function performance W_P , of Fig. 5, was obtained by considering:

$$|S_i(s)| \leq |1/w_P(s)| = \left| \frac{s + \varepsilon\omega_b}{s/M_s + \omega_b} \right|, \quad i = 1..6, \quad (15)$$

where M_s is the peak of the sensitivity function $S_i(s)$ and is a function of the closed loop damping ratio, ω_b is the close loop bandwidth. The multivariable W_P is diagonal where each entry equals a function w_P . The control output is also weighted with W_u and was obtained according to the following:

$$|(KS)_i(s)| \leq |1/w_u(s)| = \left| \frac{\varepsilon s + \omega_{bc}}{s + \omega_{bc}/M_u} \right|, \quad i = 1..6, \quad (16)$$

where M_s is the peak of the sensitivity function $S_i(s)$ and is a function of the closed loop damping ratio, ω_b is the close loop bandwidth. The obtained controller possesses a prohibitive high order of 72 and unpractical for

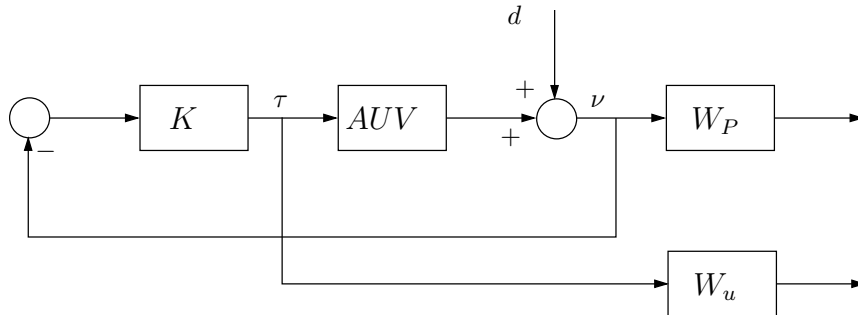


Figure 5. Augmented control system. d stands for external disturbance.

experimental implementations. This is certainly a major methodology drawback^a.

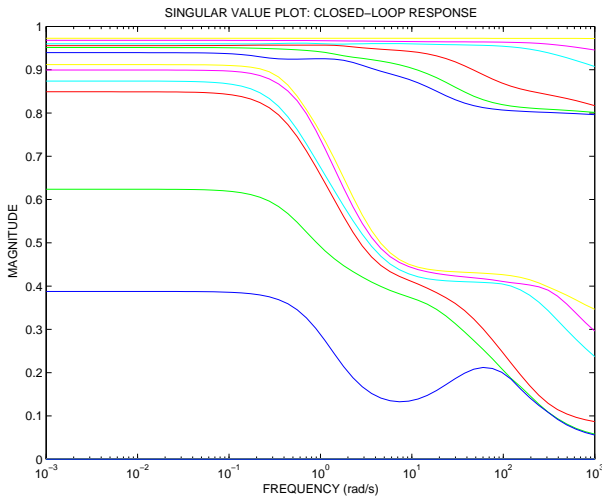
On completion of design iterations, we verified how much of the controller order could be reduced while still maintaining robust performance, i.e., checking whether $\mu_{\Delta_P}(N) < 1$ would still hold^b. Unfortunately, robust performance was not verified when decreasing the controller order by a unit. Another approach to finding a smaller order controller is to override the automatic pre-fitting algorithm for the scaling of the $D(j\omega)$ matrices and manually limit their order. This process was tested with some success making it possible to lower the controller order from 58 to 50. Reduced order designs, not considered here, may overcome this issue and render smaller order designs, refer to (Zhou and Doyle, 1998; Skogestad and Postlethwaite, 1996). Table 1 presents some results. Observe that the obtained controllers are not optimal with respect to performance, i.e. design still requires many iterations before controllers can be attained that render a closed-loop system closer to optimality. Figures 6 and 7 displays the obtained closed-loop $\bar{\sigma}(j\omega)$ and $\mu(j\omega)$ plots. Observe these plots are in accord with the those from Tab. 1. Other design schemes were tested, such as with reference command and noise signal measurement specifications. However, since performance weights tuning requires some time and many design iterations, satisfactory performance is still yet to be achieved.

^aSince the controller order equals the sum of the augmented plant's order with that of both scaling $D(j\omega)$ matrices

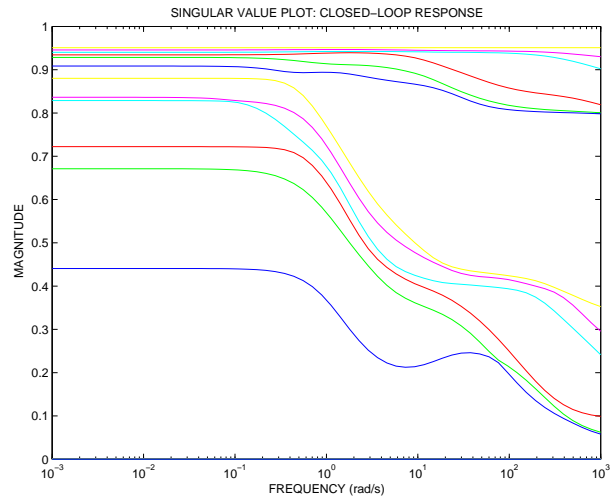
^bThis reduction is simply a truncation of the state dimension of the system matrix to a pre-determined number of states, by eliminating rows and columns of the state matrices

Table 1. Summary of some results on μ control design.

Performance Weights	W_P & W_u		W_P only	
	D Scaling	Auto-Fit.	full	semi
Peak $\mu(j\omega)$	0.974	0.968	0.958	0.987
Peak $\bar{\sigma}(j\omega)$	0.973	0.951	0.958	0.973
Iteration	16	20	16	20
Controller K order	72	56	64	52

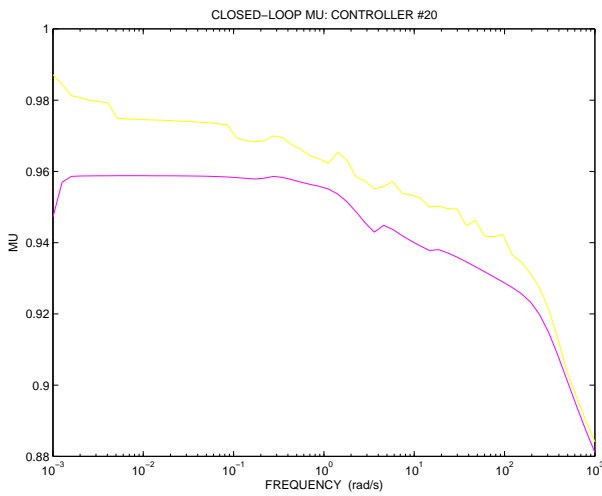


(a) Closed-loop $\bar{\sigma}$ from a W_P performance design.

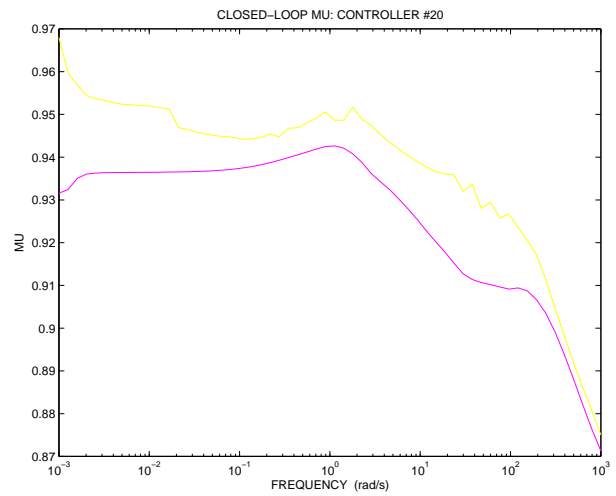


(b) Closed-loop $\bar{\sigma}$ from a W_P and W_u performance design.

Figure 6. System closed-loop maximum singular value $\bar{\sigma}$.

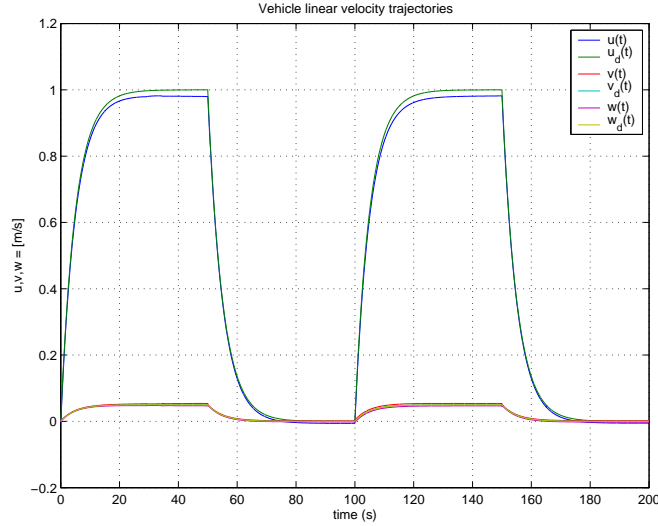


(a) Closed-loop μ from a W_P performance design.

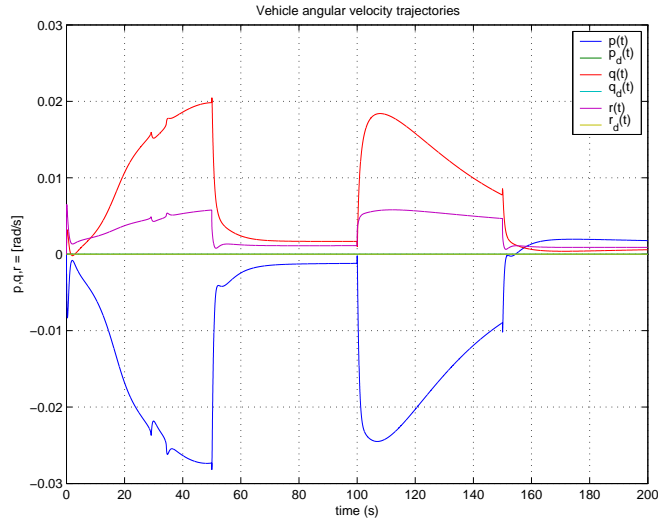


(b) Closed-loop μ from a W_P and W_u performance design.

Figure 7. System closed-loop structured singular value μ .



(a) Linear velocity tracking results with W_P .



(b) Angular velocity tracking results with W_P .

Figure 8. Velocity tracking results.

6 Simulation Results

The controller obtained was simulated with the nonlinear vehicle plant. The simulation results are shown in Fig. 8.

Reference velocity trajectories are given by pre-filtering step inputs for all *dof* with first order functions of time constants approximately close to 5s. Maximum nominal desired velocities are considered equal to $[1.00; 0.05; 0.05]m/s$ and $[0; 0; 0]rad/s$ for linear and angular motions respectively and considering simultaneous motions for all *dof*. In addition, a constant $-[1.0; 0; 0]m/s$ current velocity profile is adopted, and defined in the inertial reference system.

7 Discussions and Concluding Remarks

From the results presented above it can clearly be seen that stabilization for surge, sway and heave velocities occur in a very satisfactorily manner. Notice also, that the *2dof* scheme adopted, by using a pre-filter^c to weight step input, significantly contributed for a smooth trajectory and therefore time domain characteristics indicate absence of or small overshoot and tracking errors ($< 0.05m/s$). The observed small steady-state error was also verified with the linear plant and is attributed to the controller (synthesized with W_P after 20 iterations, refer to Tab. 1).

^cWith a cut-off frequency smaller than the CLTF bandwidth.

This note focused attention on transforming what could be considered external disturbance into easily modeled parametric perturbation. This was carried out by considering current and added mass dynamics as parametric dependent expressions with an associated uncertainty. Linear controller robust design was performed and results were obtained with a full order nonlinear plant, or AUV.

7.1 Future Implementation

This study (initial) is far from being complete and conclusive, results still need to be optimized and many questions still remain and were opened by the above considerations. Some of these could include comparisons of the above implementation with other important control schemes:

- Different current uncertainty modeling, other than parametric;
- Physical hydrodynamic parameter uncertainty modeling, in contrast to the above proposed parametric modeling;
- Current treated as external disturbance;
- Current treated part of the plant state, etc.

Further evaluation of these control strategies will be possible through experimental tests of an open-frame overactuated vehicle, currently under construction, through pool and open sea test trials.

Acknowledgements

The authors would like to thank for the sponsoring of the Coordenação do Aperfeiçoamento de Pessoal de Nível Superior - CAPES and the Financiadora de Estudos e Projetos - Finep.

References

- Balas, G. J., Doyle, J. C., Glover, K., Packard, A. and Smith, R. (2001). **μ -Analysis and Synthesis Toolbox: Users Guide**, version: 3 edn, The MathWorks Inc., The MathWorks, Inc., 3 Apple Hill Drive, Natick, MA, 01760-2098.
- Campa, G., Innocenti, M. and Nasuti, F. (1998). Robust Control of Underwater Vehicles: Sliding Mode vs. μ - Synthesis, **Proceedings of the OCEANS'98 IEEE Conference** pp. 1640–1644.
- Fossen, T. I. (1994). **Guidance and Control of Ocean Vehicles**, John Wiley & Sons.
- Ishidera, H., Tsusaka, Y., Ito, Y., Oishi, T., Chiba, S. and Maki, T. (1986). Simulation and Experiment of Automatic Controlled ROV, **Proceedings of 5th International Offshore, Mechanical and Arctic Engineering Symposium** pp. 260–267.
- Kalske, S. and Happonen, K. (1991). Motion Simulation of Subsea Vehicles, **Proceedings of the 1st International Offshore and Polar Engineering Conference, Edinburgh, UK 2**: 74–84.
- Skogestad, S. and Postlethwaite, I. (1996). **Multivariable Feedback Control: Analysis and Design**, John Wiley & Sons.
- Souza, E. C. (2003). **Modelagem e Controle de Veículos Submarinos Não Tripulados**, Dissertação (Mestrado), Escola Politécnica da Universidade de São Paulo.
- Souza, E. C., da Cruz, J. J. and Maruyama, N. (2004). The LQG/LTR Methodology for Position Control of Unmanned Underwater Vehicles, **XV Congresso Brasileiro de Automática, Gramado, RS**.
- Zhou, K. and Doyle, J. C. (1998). **Essentials of Robust Control**, Prentice Hall.

Responsibility Notice

The authors are the only responsible for the printed material included in this paper.